Effect of Inter- and Intra-annual Thermohaline Variability on Acoustic Propagation

Peter C Chu, Colleen McDonald, Murat Kucukosmanoglu
Albert Judono, Tetyana Margolina

Department of Oceanography
Naval Postgraduate School

pcchu@nps.edu
http://faculty.nps.edu/pcchu/

SPIE Defense + Security 2017 Conference, Anaheim, California, 9-13 April 2017

OPNAV N97/N2N6E Interest

How can inter- and intra-annual variability in the ocean be leveraged by the submarine Force?

Outline

- (1) Introduction
- (2) Optimal Spectral Decomposition (OSD)
- (3) Synoptic Monthly Gridded World Ocean Database (WOD) → Interannual Variability
- (4) Impact on Acoustical Propagation
- (5) Conclusions

(1) Introduction

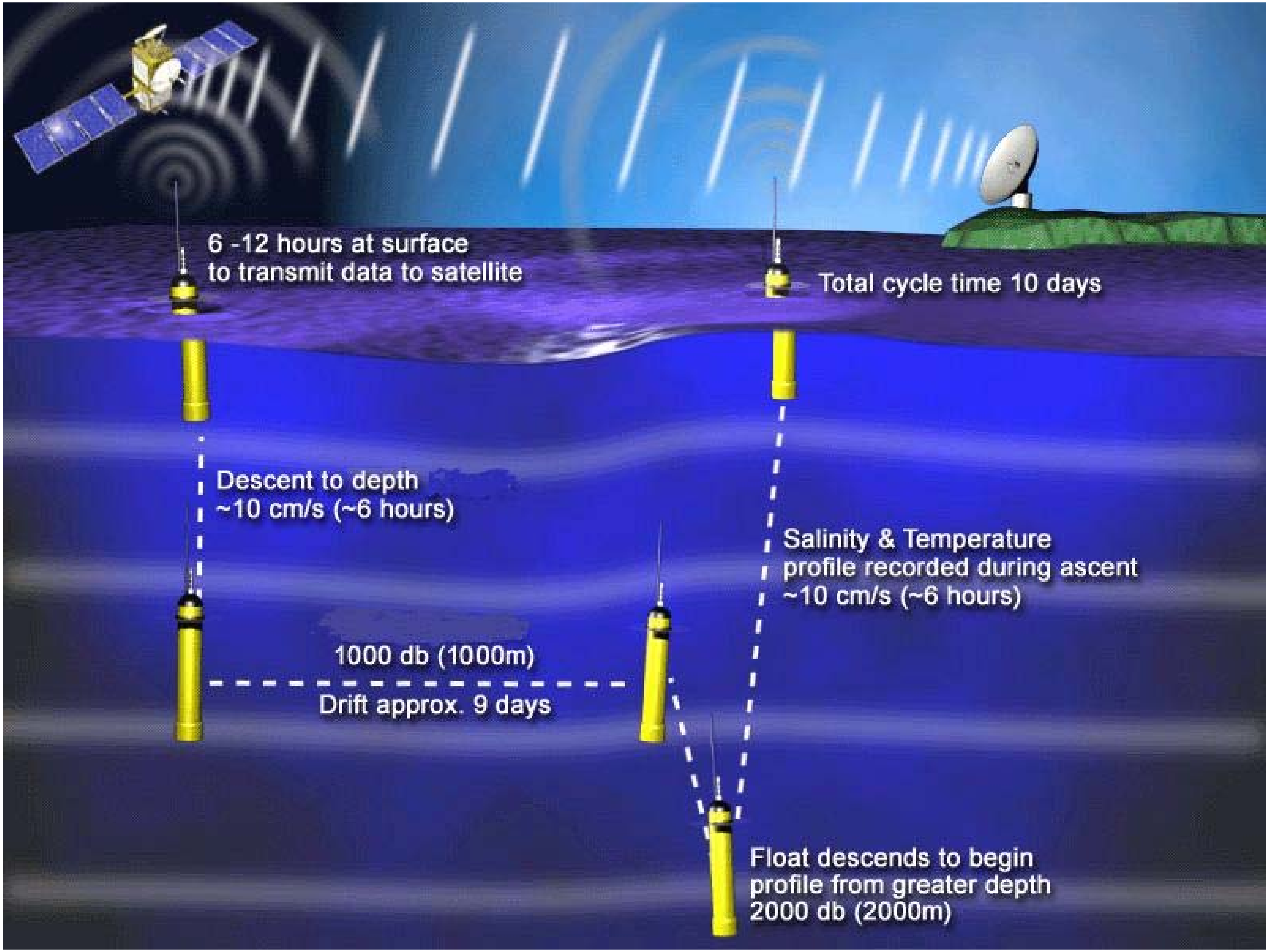
6 -12 hours at surface
to transmit data to satellite
Total cycle time 10 days
Descent to depth
~10 cm/s (~6 hours)
Salinity & Temperature
profile recorded during ascent
~10 cm/s (~6 hours)
1000 db (1000m)
Drift approx. 9 days
Float descends to begin
profile from greater depth
2000 db (2000m)

Argo – Part of the Integrated Global Observation Strategy

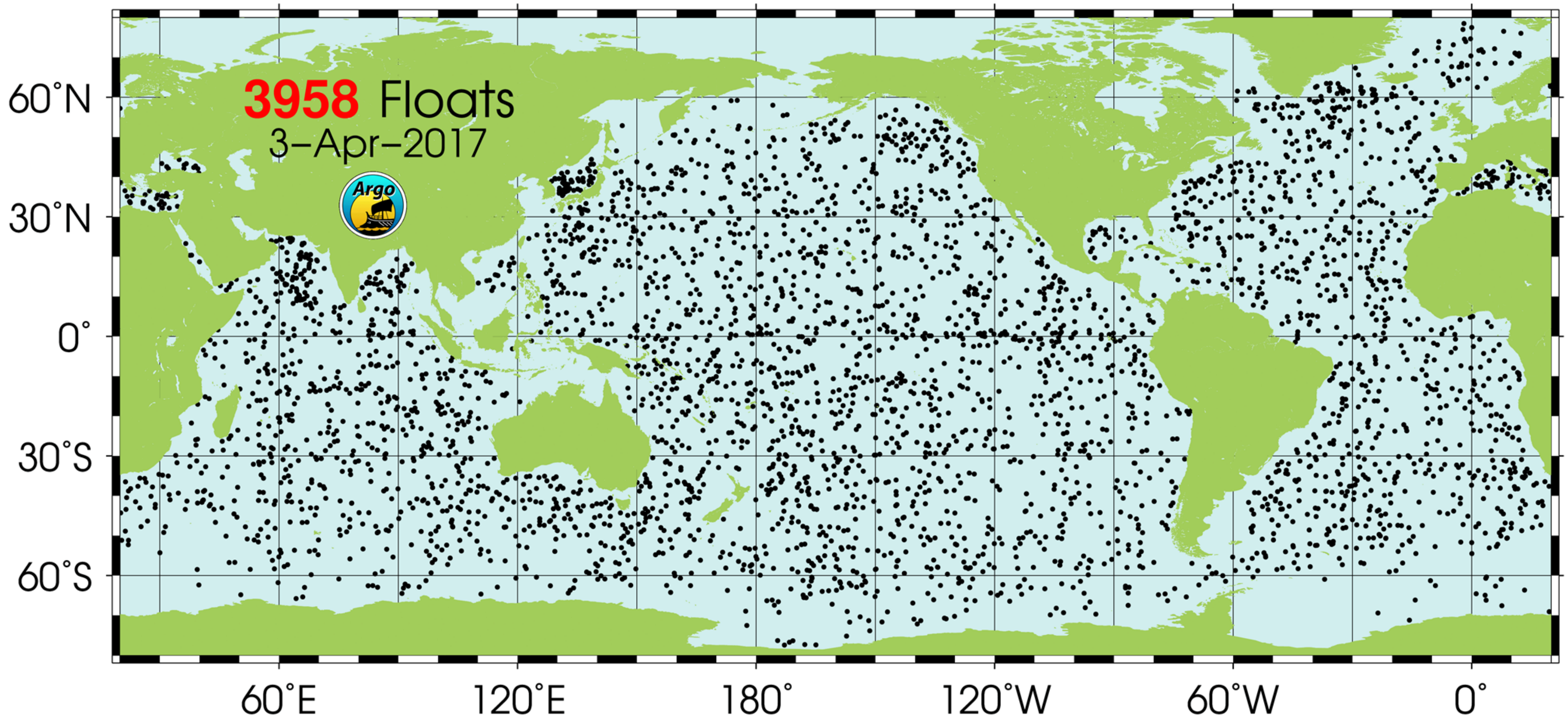

Instrumentation on Glider

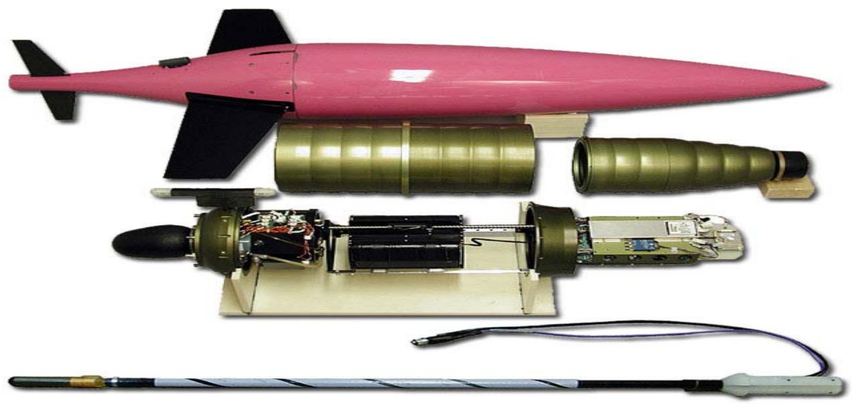

From SEAGLIDER Fabrication Center. seaglider.washington.edu

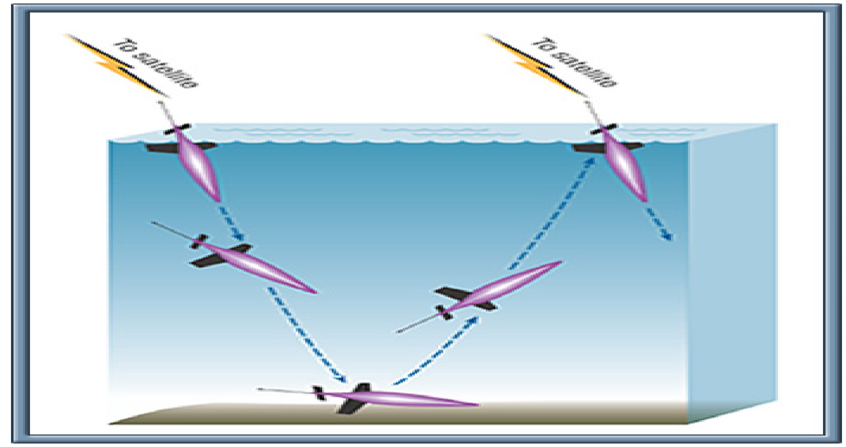

From Applied Physics Laboratory www.apl.washington.edu

- Profiles from surface to 1500m
- Buoyancy engine produces slight buoyancy changes to induce pitched upward or downward gliding. Internal battery pack is shifted side to side to facilitate turning.
- Uses Iridium LEO system to obtain GPS fixes, upload data, and receive command and control instructions from NAVO Glider Operations Center (GOC).

Instrumentation

1) Seabird Electronics' SBE 41 CTD sensor
- 1 Hz sample rate
- T accurate to .001 degrees C
- Salinity accurate to .005 PSU*
- Pressure accurate to 2 dbar*

2) WET Labs, Inc ECO bb2fl optical sensor
- Optical Backscatter @ 470nm and 650nm*
- Fluorimeter: Chlorophyll-A @ 470 nm*
- Samples in top 300m to preserve battery life

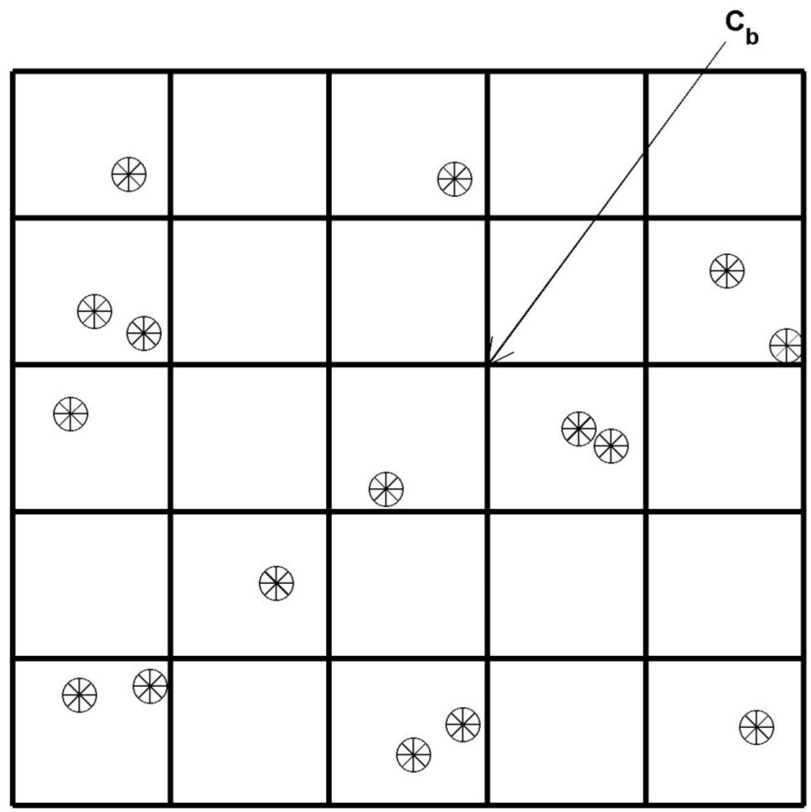

Ocean data assimilation with $\boldsymbol{c}_b$ located at the grid points, and $\boldsymbol{c}_o$ located at the points '*". The ocean data assimilation is to convert the innovation, $\boldsymbol{d} = \boldsymbol{c}_o - \mathbf{H}\boldsymbol{c}_b$, from the observational points to the grid points.

Assimilated Variable $\mathbf{c}(\mathbf{x}, z, t)$

$\mathbf{c}_t$ → "true"

$\mathbf{c}_a$ → analysis (assimilated)

$\mathbf{c}_b$ → background (modeled)

$(\mathbf{c}_t, \mathbf{c}_a, \mathbf{c}_b)$ → grid points → $\mathbf{r}_n$ → total N

$\mathbf{c}_o$ → Observation → Obs points → $\mathbf{r}^{(m)}$

→ total M

Traditional Ocean Data Assimilation Schemes

- Optimal Interpolation (OI)
- Kalman Filter
- Variational Methods

Data Assimilation

$$\mathbf{c}_a = \mathbf{c}_b + \mathbf{W}\mathbf{d}$$

Innovation → $\mathbf{d} = \mathbf{c}_o - \mathbf{H}\mathbf{c}_b$

Various ways → **W** – Weight Matrix
→ Different Data Assimilation Schemes

H =[h_{mn}] → the $M \times N$ linear observation operator matrix

W → Depends on **B**, **R**

B → Background Error Covariance Matrix

R → observational error covariance matrix (usually assumed given)

Background Error Covariance Matrix B & Observational Error Covariance Matrix R

$$\boldsymbol{\varepsilon}_a = \mathbf{c}_a - \mathbf{c}_t, \quad \boldsymbol{\varepsilon}_o \equiv \mathbf{H}^T \mathbf{c}_o - \mathbf{c}_t$$

$$E^2 = \left\langle \boldsymbol{\varepsilon}_a^T \boldsymbol{\varepsilon}_a \right\rangle \rightarrow \min$$

$$\partial E^2 / \partial w_{nm} = 0$$

- Optimal Interpolation (OI) $\quad \mathbf{W} = \mathbf{B}\mathbf{H}^T(\mathbf{R} + \mathbf{H}\mathbf{B}\mathbf{H}^T)^{-1}$
- Kalman Filter (KF) $\quad \mathbf{W}_i = \mathbf{B}^f(t_i)\mathbf{H}^T[\mathbf{R}_i + \mathbf{H}_i\mathbf{B}^f(t_i)\mathbf{H}^T]^{-1}$
- Variational Method $\quad \mathbf{W} = (\mathbf{B}^{-1} + \mathbf{H}^T\mathbf{R}^{-1}\mathbf{H})^{-1}\mathbf{H}^T\mathbf{R}^{-1}$

Effectively using the ocean topographic characteristics

↓

A new spectral ocean data assimilation method without requiring *a priori* knowledge of matrix B

(2) OSD Method

References

- Chu, P.C., C.W. Fan, and T. Margolina, 2016: Ocean spectral data assimilation without background error covariance matrix. *Ocean Dynamics*, 66, 1143-1163.
- Chu, P.C., R.T. Tokmakian, C.W. Fan, and C.L. Sun, 2015: Optimal spectral decomposition (OSD) for ocean data assimilation. *Journal of Atmospheric and Oceanic Technology*, **32**, 828-841.
- Chu, P.C., 2011: Global upper ocean heat content and climate variability. *Ocean Dynamics*, **61** (8), 1189-1204.
- Chu, P.C., L.M. Ivanov, O.V. Melnichenko, and N.C. Wells, 2007: Long baroclinic Rossby waves in the tropical North Atlantic observed from profiling floats. *Journal of Geophysical Research*, **112**, C05032, doi:10.1029/2006JC003698.
- Chu, P.C., L.M. Ivanov, T.P. Korzhova, T.M. Margolina, and O.M. Melnichenko, 2003: Analysis of sparse and noisy ocean current data using flow decomposition. Part 2: Application to Eulerian and Lagrangian data. *Journal of Atmospheric and Oceanic Technology*, **20**, 492-512.
- Chu, P.C., L.M. Ivanov, T.P. Korzhova, T.M. Margolina, and O.M. Melnichenko, 2003: Analysis of sparse and noisy ocean current data using flow decomposition. Part 1: Theory. *Journal of Atmospheric and Oceanic Technology*, **20** (4), 478-491.

Basis Functions

$$\nabla^2\phi_k = -\lambda_k \phi_{\mathrm{k},} \quad \left[b_1 \mathbf{n} \bullet \nabla \phi_k + b_2 \phi_k \right]|_\Gamma = 0, \quad k = 1, \ldots, \infty$$

ϕ_k → The eigen functions of the 2D Laplacian Operator

satisfaction of the same homogeneous boundary condition of the assimilated variable anomaly

$b_1 = 0$ → Dirichlet boundary condition

$b_2 = 0$ → Newmann boundary condition

$b_1 \neq 0, \; b_2 \neq 0$ $\rightarrow$ Cauchy boundary condition

Basis Function Matrix

Φ Matrix →

$$\boldsymbol{\Phi} = \{\phi_{kn}\} = \begin{bmatrix} \phi_1(\mathbf{r}_1) & \phi_2(\mathbf{r}_1) & \dots & \phi_K(\mathbf{r}_1) \\ \phi_1(\mathbf{r}_2) & \phi_2(\mathbf{r}_2) & \dots & \phi_K(\mathbf{r}_2) \\ \dots & \dots & \dots & \dots \\ \phi_1(\mathbf{r}_N) & \phi_2(\mathbf{r}_N) & \dots & \phi_K(\mathbf{r}_N) \end{bmatrix}$$

K → truncated mode number

N → number of grid points

First 12 basis functions
for the Pacific Ocean
at the surface.

DBDB5

Dirichlet boundary
condition at the southern
boundary (Antarctic),

Newmann boundary
condition elsewhere

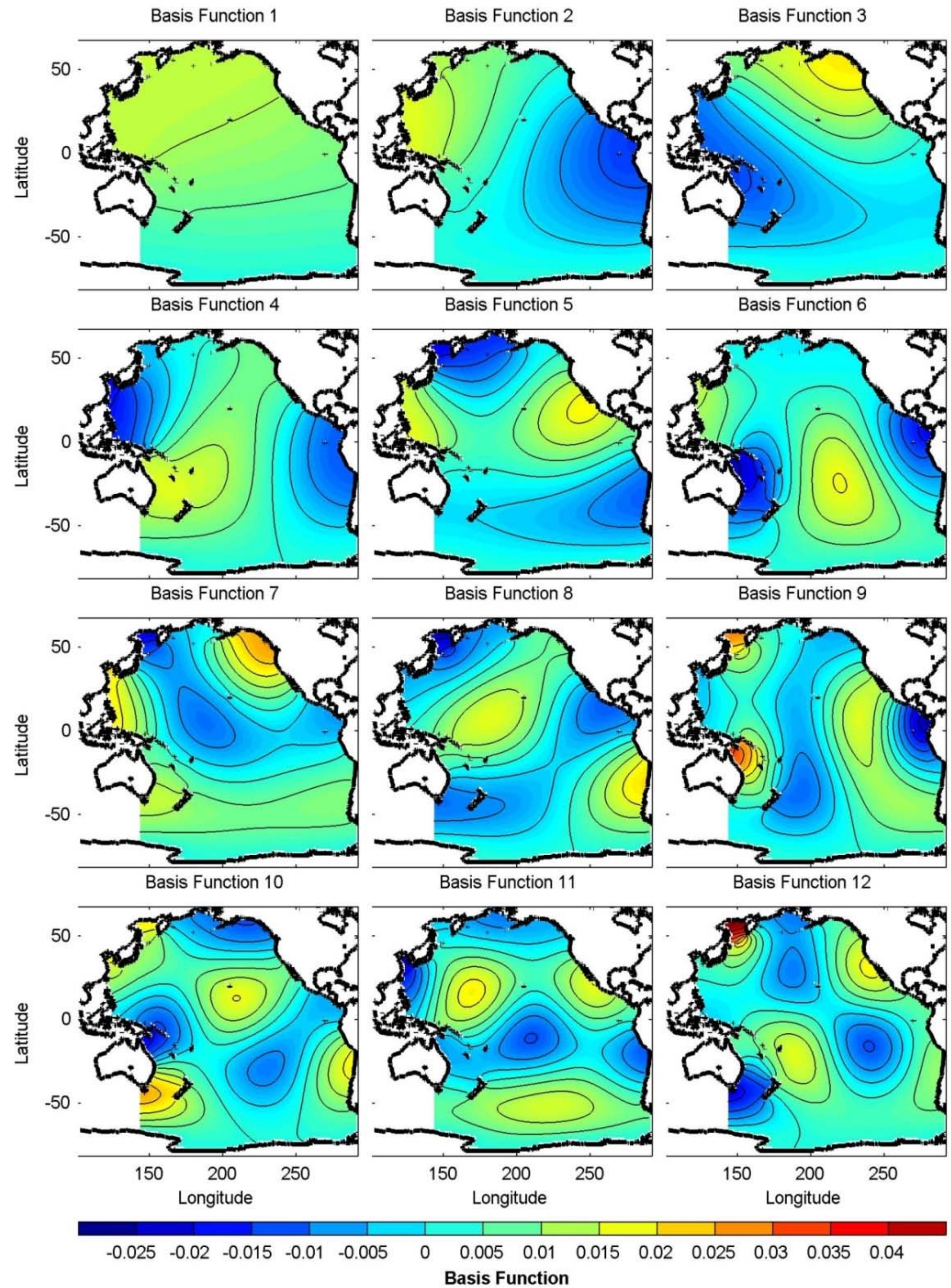

Spectral Ocean Data Assimilation

$$\mathbf{c}_a = \mathbf{c}_b + f_n \mathbf{s}^{(K)}, \quad s_K(\mathbf{r}_n) \equiv \sum_{k=1}^{K} a_k \, \phi_k(\mathbf{r}_n),$$

$\mathbf{H} = [h_{mn}]$ → the $M \times N$
linear observation operator matrix

$$f_n \equiv \sum_{m=1}^{M} h_{nm}$$

$$\mathbf{F} = \begin{bmatrix} f_1 & 0 & 0 & 0 & 0 & 0 \\ 0 & f_2 & 0 & 0 & 0 & 0 \\ 0 & 0 & \ddots_i & 0 & 0 & 0 \\ 0 & 0 & 0 & f_n & 0 & 0 \\ 0 & 0 & 0 & 0 & \ddots & 0 \\ 0 & 0 & 0 & 0 & 0 & f_N \end{bmatrix}$$

$$\boldsymbol{\varepsilon}_a \equiv \mathbf{c}_a - \mathbf{c}_t = (\mathbf{c}_a - \mathbf{c}_b) + (\mathbf{c}_b - \mathbf{c}_t) = \boldsymbol{\varepsilon}_K + \boldsymbol{\varepsilon}_o$$

$$\boldsymbol{\varepsilon}_K \equiv \left[f_n \mathbf{s}^{(K)} - \mathbf{H}^T(\mathbf{c}_o - \mathbf{H}\mathbf{c}_b) \right], \qquad \boldsymbol{\varepsilon}_o \equiv \mathbf{H}^T \mathbf{c}_o - \mathbf{c}_t \qquad \left\langle \boldsymbol{\varepsilon}_o^T \boldsymbol{\varepsilon}_K \right\rangle = 0$$

$$E^2 = \left\langle \boldsymbol{\varepsilon}_a^T \boldsymbol{\varepsilon}_a \right\rangle = E_K^2 + E_o^2, \quad E_K^2 \equiv \left\langle \boldsymbol{\varepsilon}_K^T \boldsymbol{\varepsilon}_K \right\rangle, E_o^2 \equiv \left\langle \boldsymbol{\varepsilon}_o^T \boldsymbol{\varepsilon}_o \right\rangle$$

OSD Data Analysis/Assimilation

$$E^2 \to \min, \quad \partial E^2 / \partial a_k = \partial E^2_{K_{OPT}} / \partial a_k = 0, \quad k = 1, \ldots, K_{OPT}$$

$$E_K^2 = \sum_{n=1}^{N} \left(f_n \sum_{k=1}^{K_{OPT}} a_k \phi_{kn} - D_n \right)^2 \to \min$$

$$\sum_{k'=1}^{K} \sum_{n=1}^{N} (\phi_{kn} f_n \phi_{nk'}) a_{k'} = \sum_{n=1}^{N} \phi_{kn} f_n D_n, \qquad k = 1,\, 2,\, \ldots,\, K_{OPT}$$

$$\mathbf{\Phi F \Phi}^T \mathbf{A} = \mathbf{\Phi F D}, \qquad \mathbf{A} = \left[\mathbf{\Phi F \Phi}^T \right]^{-1} \mathbf{\Phi F D}$$

OSD → $\mathbf{c}_a = \mathbf{c}_b + \mathbf{F \Phi}^T \left[\mathbf{\Phi F \Phi}^T \right]^{-1} \mathbf{\Phi H}^T \mathbf{d}$

No Background Error Covariance Matrix Needed

(3) Synoptic Monthly Gridded World Ocean Database (SMG-WOD)

- (1) Synoptic monthly gridded three dimensional (3D) World Ocean Database temperature and salinity from January 1945 to December 2014, **NOAA National Centers for Environmental Information** (NOAA/NCEI Accession 0140938) download
- (2) Synoptic Monthly Gridded WOD Absolute Geostrophic Velocity (SMG-WOD-V) (January 1945 - December 2014) with the P-Vector Method, **NOAA National Centers for Environmental Information** (NOAA/NCEI Accession 0146195) download
- (3) Synoptic monthly gridded Global Temperature and Salinity Profile Programme (GTSPP) water temperature and salinity from January 1990 to December 2009, **NOAA National Centers for Environmental Information** (NOAA/NCEI Accession 0138647) download
- (4) Synoptic monthly gridded (0.25^{o}) three dimensional (3D) Mediterranean Sea (T, S, u, v) dataset (January 1960 - December 2013) from the NOAA/NCEI WOD Profile Data, **NOAA National Centers for Environmental Information** (NCEI Accession 0157702)
- (5) Synoptic monthly gridded (0.25^{o}) three dimensional (3D) Japan/East Sea (T, S, u, v) dataset (January 1960 - December 2013) from the NOAA/NCEI WOD Profile Data, **NOAA National Centers for Environmental Information** (NCEI Accession 0157703)
- (6) Synoptic monthly gridded (0.25^{o}) Gulf of Mexico (T, S, u, v) dataset (January 1945 - December 2014) from the NOAA/NCEI WOD Profile Data, **NOAA National Centers for Environmental Information** (NOAA/NCEI Accession 0156423) download

Mediterranean Sea Sediments

A : 1000 m Clay, B: ~200 m, Very Fine Sand
C: 1000 m Sandy Mud, D: 1000 m Very Fine Silt
E: ~70 m Sandy Mud

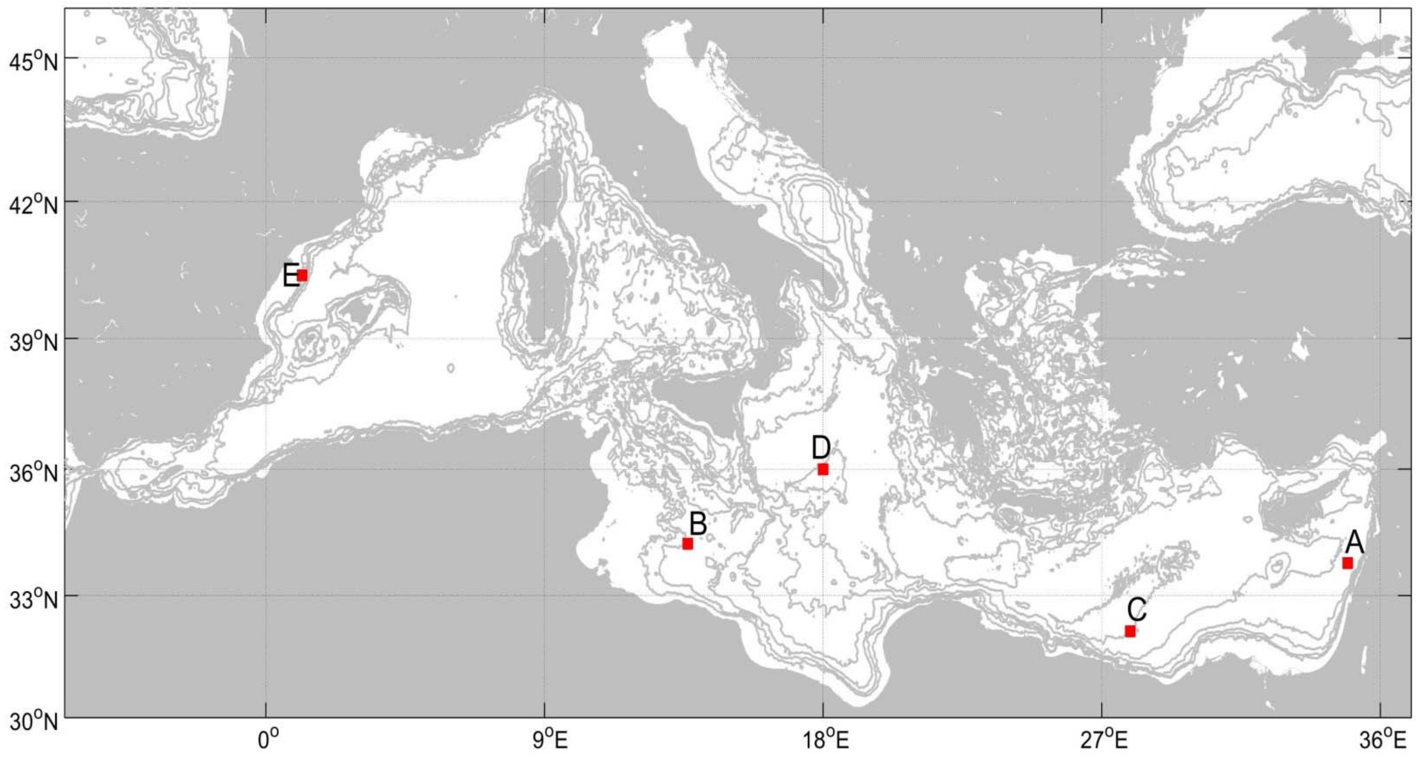

Interannual Variability – at Point A

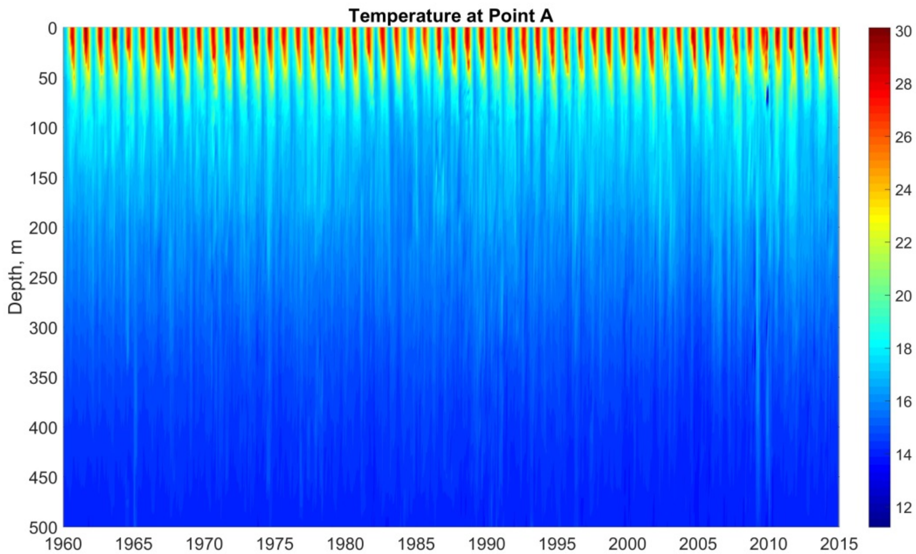

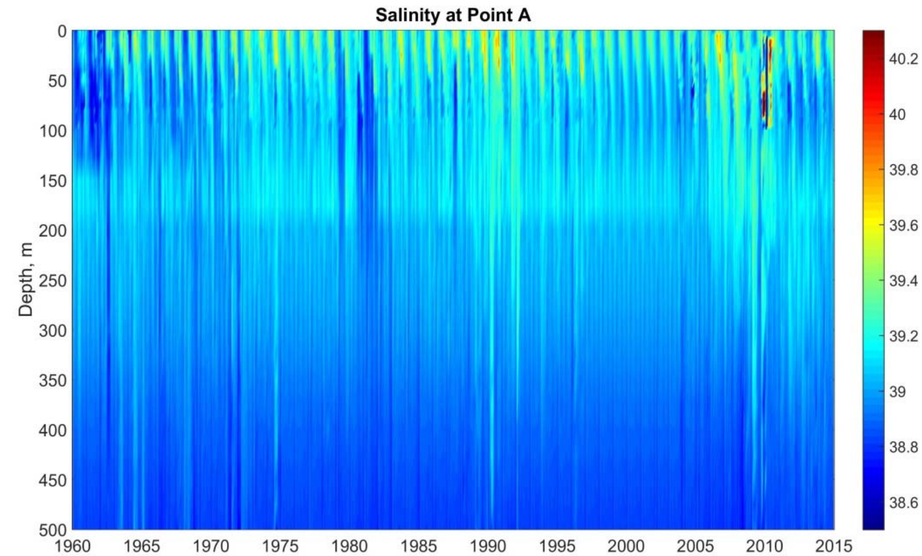

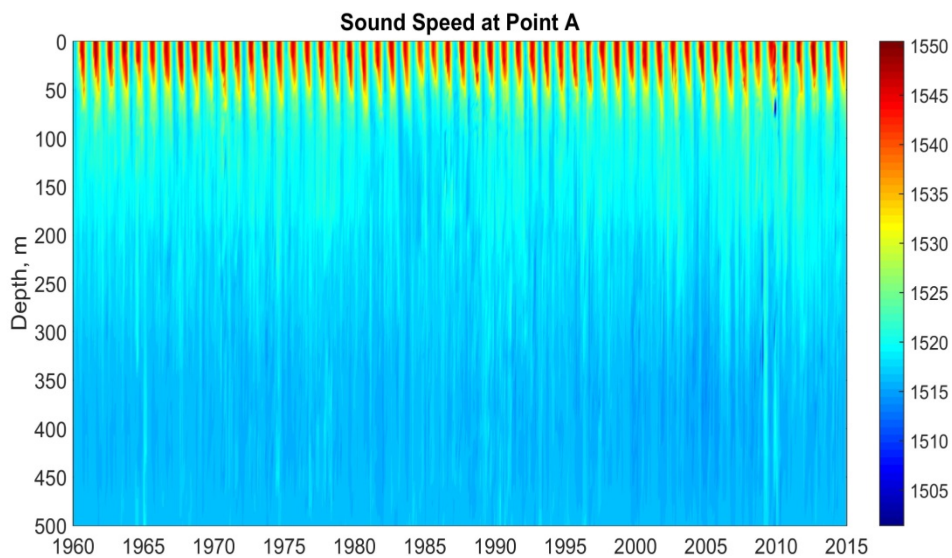

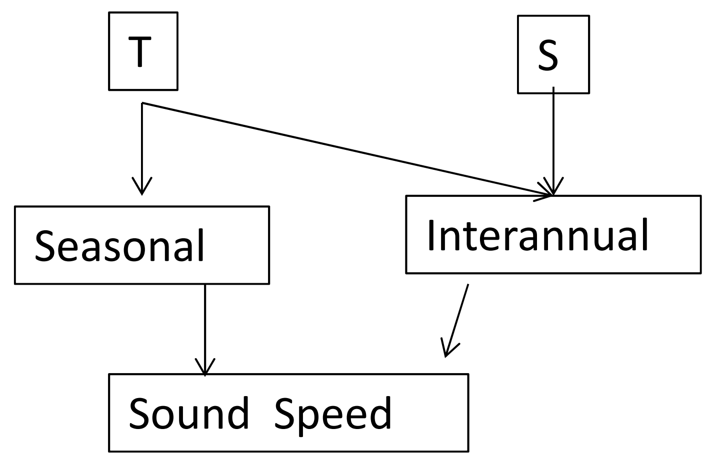

(4) Impact on Acoustic Propagation

BELLHOP –Ray Trace Model

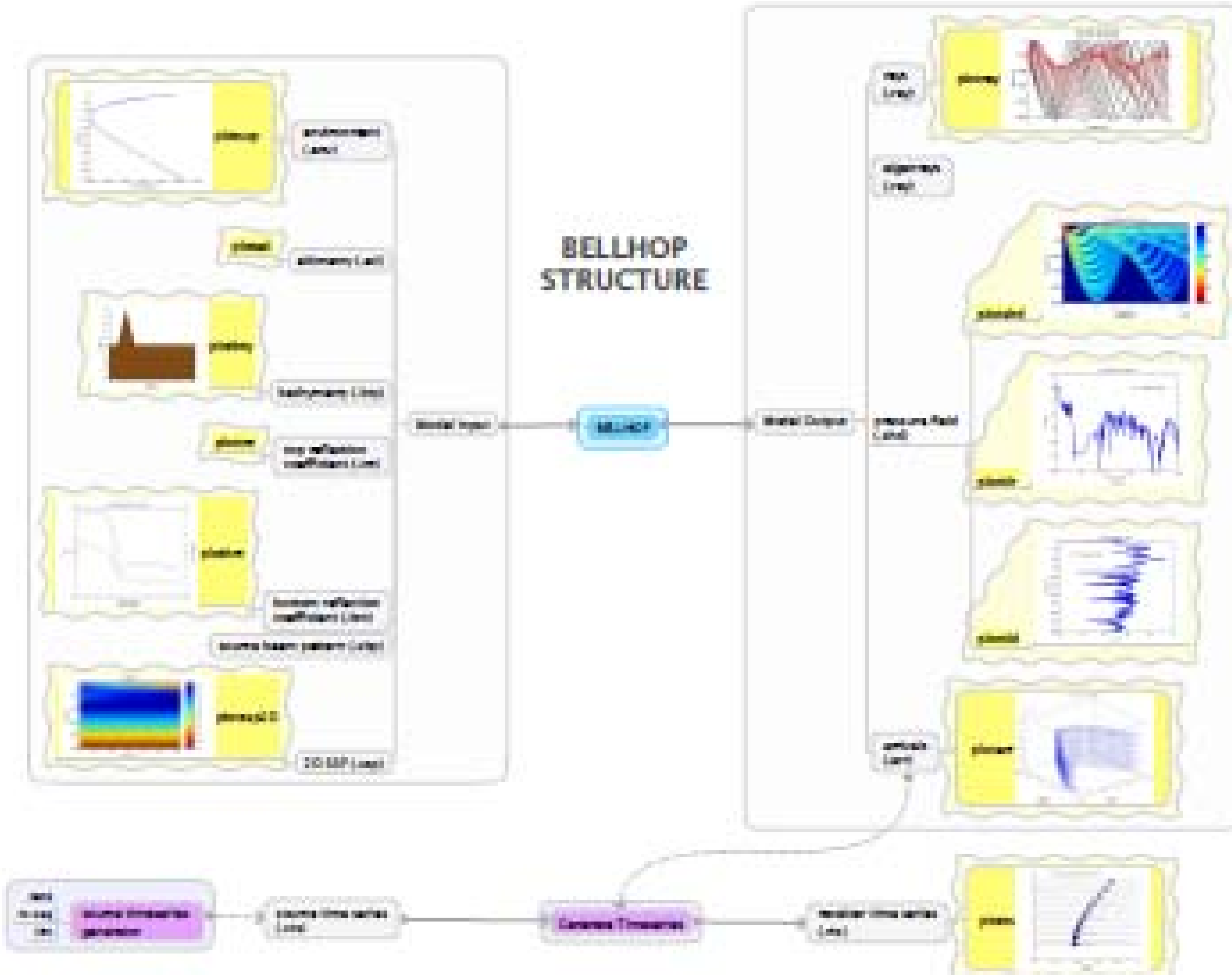

Bellhop Model Setup

• Sound Source Depth	40 m
• Source Frequency	3500 Hz
• Maximum range	70 nmi
• Bathymetry	DBDB-NAVO
• Sediments	High Frequency Environmental Acoustics (HFEVA)
• Ray direction	Eastward

Point A January in the 1980-1990 (left) and in the 2000-2014 (right)

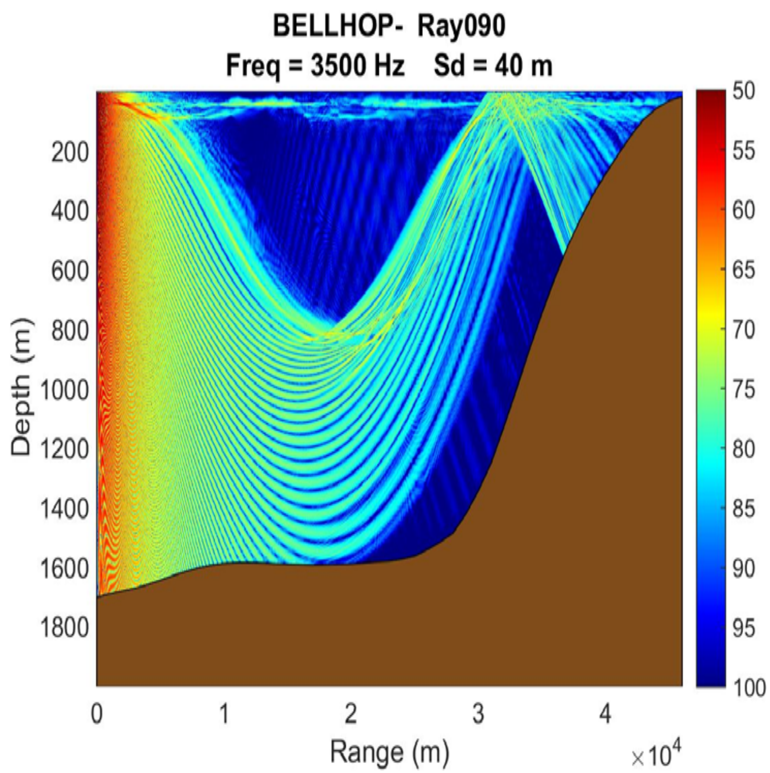

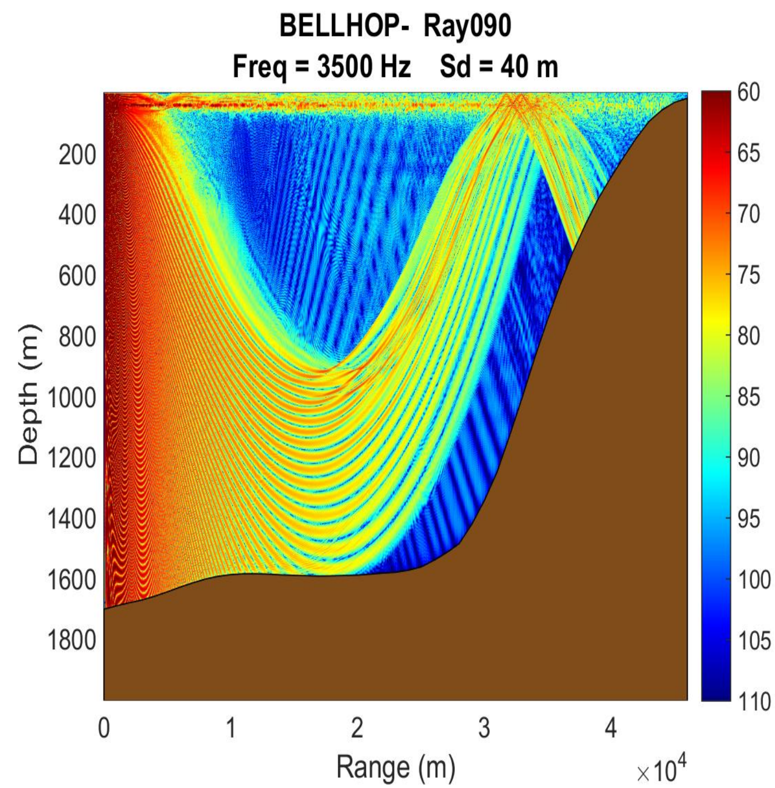

Point A August in the 1980-1990 (left) and in the 2000-2014 (right)

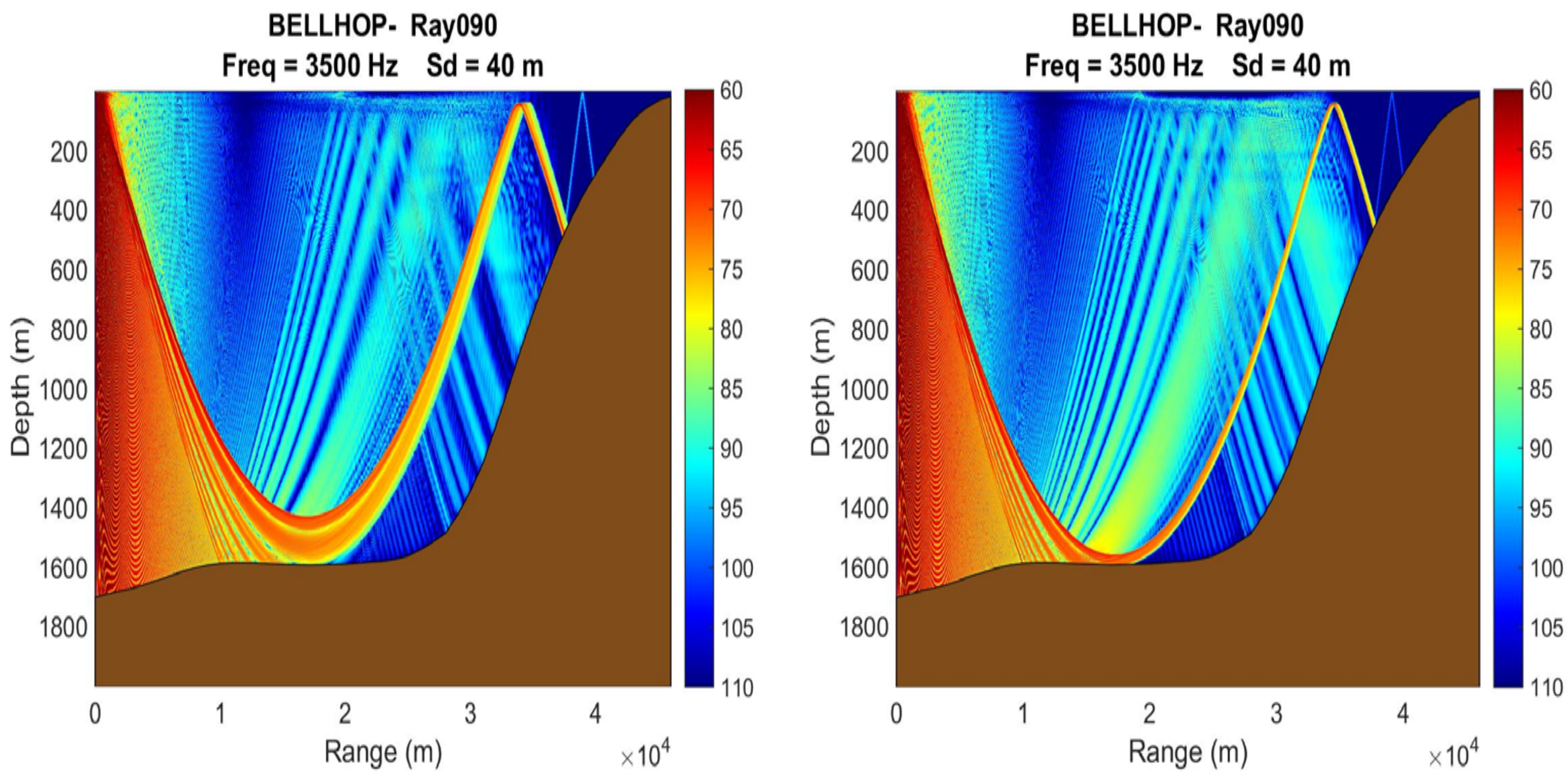

Conclusions

- SMG-WOD provides intra- and inter-annual variability of the (T, S) fields and in turn of the sound speed.
- Impact of the inter- and intra-annual variability in the ocean on the acoustic transmission can be leveraged by the submarine Force.

Acknowledgement

- This project is sponsored by N97/N2N6E through the NPS Naval Research Program (NRP)
- Topic Sponsor:

  Dr. Andrew Greene

  Oceanography Technical Director

  OPNAV N97